Adsorption of Methylene Blue Dye using synthesized Copper-keratin nanoparticles from sheep hooves

Cheptoo Caroline[a], Wycliffe C. Wanyonyi[a], Joyce J. Kiplimo[a], Edwin S. Madivoli[b], Sammy Wanakai[b], Peter Olusakin Oladoye[c]

[a]*Department of Mathematics, Actuarial and Physical Sciences, University of Kabianga, P.O. Box 2030, 20200 Kericho, Kenya*
[b]*Department of Chemistry, Jomo Kenyatta University of Agriculture and Technology PO BOX 62000 – 00200, Nairobi, Kenya*
[c]*Department of Chemistry and Biochemistry, Florida International University, Miami 33199, United States.*

ABSTRACT

Copper nanoparticles were synthesized using keratin extracted from sheep hooves as a reducing and stabilizing agent. The synthesized nanoparticles were analyzed using UV-VIS, FT-IR, SEM and XRD. Formation of CuNps was manifested by color adjustment from blue to violet. Surface polariton peaks at 313 and 544 nm established existence of CuNps. FT-IR measurements on CuNps indicated peaks associated with O-H, C=C, C-O groups. XRD measurement revealed FCC crystalline structure of CuNps. SEM measurements showed sphere-shaped particles of size ranging between 2.0 -16.0 nm. The nanoparticles obtained were applied in adsorption of methylene blue (MB) dye from aqueous solution. Adsorption of MB dye by Copper nanoparticles highly depended on sorption time, dosage of copper nanoparticles, temperature, initial pH and dye concentration. Equilibrium for removal of methyl blue at 25 °C was attained after 330 min with efficiency of 95 % removal of the dye attained. Both Langmuir and Freundlich isotherm were almost equal signifying that both models could describe adsorption process at room temperature (25°C). Pseudo second order kinetics was suitable in describing sorption process while adsorption isotherms revealed that the process followed Temkins isotherm model.

Keywords: Methylene blue; Copper-keratin nanoparticles; Kinetics; Adsorption; pollution

1. INTRODUCTION

Synthetic dyes are broadly applied in printing, fuel-marking, paper, plastics, cosmetic and leather industries [1,2]. It has been reported that that dyes and pigments produced per year exceeds 0.7 million tonnes from which 2-15% of the dye is lost in waste water during industrial processes [3]. Waste water from industries contaminate ground water and surface water bodies posing danger to aquatic plants, animals and humans using the contaminated water since the dyes are non-biodegradable, mutagenic and toxic [4]. Due to diverse molecular structural chromophore, dyes are resilient to degradation by microbial, chemical and physical methods. Metabolites resulting from degradation might also be mutagenic, toxic and carcinogenic [5]. Dye contamination obstruct growth of bacteria, lowers dissolved oxygen suffocating aquatic animals

Preprint not peer reviewed

This preprint research paper has not been peer reviewed. Electronic copy available at: https://ssrn.com/abstract=4957961

in severe cases and slow down photosynthesis of aquatic plants, by reducing intensity of light getting to the plants [4].

Methylene blue ($C_{16}H_{18}N_3ClS$ and 319.85 g/mol) (Fig. 1), is an organic dark green dye powder which disassociate in water to produce a blue solution [6]. The dye which extensively consumed in textile industry as coloring agent for fibers is blamed for serious health risks such as central nervous system disorder, teratogenic, carcinogenic, embryo toxic, respiratory disorder, gastrointestinal, dermatological and genitourinary complications amongst others [6–9]. Different technologies including biological, chemical techniques, ion exchange, screening, coagulation, physisorption among others have been employed in dye removal from aquatic environment [3]. These methods can be complex or uneconomical due to nature of technology used use of specific equipment [10]. Chemical methods may cause secondary pollutants which require further treatment [11]. Physical methods include membrane based technology which suffers the downsides which include membrane denaturation and bore congestion [12]. Adsorption is the most versatile method which gives the good results in sorption of organic dyes from waste water [13]. Nanoparticles have gained more attention in technological development compared to their macro sized counterparts. The unique properties of nanomaterial are as a result of their nano-scale size and shape.

In effort to stamp out environmental pollution posed keratinous waste and colored wastewaters contaminated by organic dyes, this study affords the opportunity to synthesize Copper-keratin nanoparticles from sheep hooves for sorption of MB dye. Nanoparticles are advantageous in adsorption since they provide greater sorption capability owing to the larger surface area because of their small particle size [14]. This study offers a golden chance to advance an alternate technology for exploiting plentiful keratinous solid waste in resolving environmental plight in our concerted strive to achieve high performing, low cost and versatile adsorbent for adsorption of organic coloration from contaminated wastewaters.

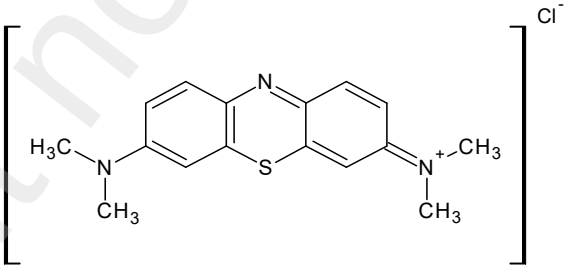


Fig. 1. Structure of Methylene Blue Dye

2. MATERIALS AND METHODS

2.1 Chemicals and reagents

Chemicals used in this work were procured from Ranbaxy Chemicals, Nairobi Kenya, were of the utmost analytical grade and applied without more purification. Distilled water was used to prepare working solutions while the required pH was achieved by either adding a few drops 0.20 M NaOH or 0.20 M HCL. Hanna pH meter model HI98128 was used to monitor the pH values.

Preprint not peer reviewed

This preprint research paper has not been peer reviewed. Electronic copy available at: https://ssrn.com/abstract=4957961

2.2 Extraction of Keratin, Synthesis and Characterization of Copper nanoparticle

Hooves collected from slaughter house in in Litein town, Kericho County in Kenya. They were washed numerous times using clean water and detergent to get rid of soil, dirt and foreign particles. They were rinsed using distilled water followed by 70 % ethanol, dried out for 24 hours at 50 °C in an oven and pulverized. 50 g of hooves powder were defatted using 500ml of hexane and dichloromethane (1:1 v/v) mixture for 24 hours. Defatted hooves were cleaned with distilled water, transferred into 800 ml pyrex glass and treated with 500 ml of 2.5 w/v % NaOH and heated in a water path set at 80 °C for 2 hours. The mixtures were filtered to remove any undissolved solid and pH adjusted to 3.8 using 0.2 M HCl to obtain keratin precipitate.

Synthesis of Copper nanoparticles was done by adding 1 g of keratin to 50 ml of 0.01 M $CuSO_4$ in Erlenmeyer flask and sealed using aluminum foil to prevent spillage. The mixture was shaken using orbital shaker (GS-20 AKMLab Orbital Shaker) set at 25 °C and 140 rpm for 10 minutes. To the mixture, 15 ml of 2 M NaOH was added with continuous shaking at 140 rpm for 30 minutes and transferred to a water path at 80 °C where it was heated for 90 min to obtain copper nanoparticles. The nanoparticles were decanted after 24 hours, cleaned with water, washed with ethanol and filtered using whatman filter no1. They were further air dried and stored in a clean vial for use in adsorption experiments. Optical properties of copper nanoparticles were assessed using UV-VIS spectrophotometer (UV-1800 Shimadzu UV spectrophotometer). Functional groups on the CuNps were examined by FTIR instrument (IRAffinity-1S FTIR-Shimadzu model) while XRD measurement on CuNps was carried out using Cu Kα radiation. Magnitude dispersal and morphology was determined by Scanning Electron Microscope (SEM MIRA3 TESCAN)

2.3 Adsorption Experiment

Adsorption experiments for methylene blue (MB) were studied in batch experiment by investigating the impact of time, initial pH (2-13), dye concentration, dosage of copper nanoparticles and temperature. Specific amount of copper nanoparticles were mixed with 10 ml of dye solution of a predetermined MB concentration. Aliquots were drawn at various intervals of time and analysed using UV-VIS spectrophotometer to ascertain the residual MB at (λ_{max} = 664 nm). Impact of contact time was inspected using 8 mg of nanoparticles and 10 ml of 5ppm of MB dye solution. Effect of nanoparticles dose was investigated using 1, 2, 4, 6, 8 and 10 mg of copper nanoparticles in10 ml of 5 ppm MB dye solution. Influence of temperature and pH was investigated using 10 ml of 5ppm MB and 8 mg of copper nanoparticles. Dye concentration effect was scrutinized by changing MB concentration from 10 ppm to 0.625 ppm while using 10 ml of the dye and 8 mg of copper nanoparticles. Aliquots of the dye solution with a volume of 3.0 ml was taken at predetermined time interims of 30 minutes and analyzed to ascertain remaining dye concentration using UV-VIS spectrophotometer. Quantity of MB removed by copper nanoparticles in (mg/g) was determined using equ 1.

$$q_e = \frac{V(C_\circ - Ce)}{W} \quad (1)$$

Efficiency of the dye removal by copper nanoparticles was calculated using equ 2:

This preprint research paper has not been peer reviewed. Electronic copy available at: https://ssrn.com/abstract=4957961

$$\% \text{ of Dye removed} = \frac{C_\circ - C_e}{C_\circ} * 100 \quad (2)$$

Where C_o and C_e are the initial and equilibrium MB concentration (mg-l), V is the volume of MB dye (L) and W is the amount of CuNps (g). Adsorption kinetics of MB was studied using varied dye concentrations at room temperature (25°C). 8.0 mg of copper nanoparticles was added to 10 mL MB solution in a 50 mL conical flask set at 140 revolutions per minute. Dye solution were drawn from the flask at an interval of 20 minutes to determine MB dye concentration and then returned to restore initial volume.

3. RESULTS AND DISCUSSION

3.1 Optimization of KE-CuNPs Synthesis

3.1.1 Effect of time on synthesis of KE-CuNPs

The length of incubation time affects type and quality of nanoparticles synthesized using green methods [15]. Influence of time on synthesis of copper nanoparticle was tracked using UV-VIS spectrophotometer and the findings displayed in Fig. 2 (a). Nanoparticles yield surged with rise in time until 90 minutes when saturation was attained. Further increase in time resulted in decreased of nanoparticles concentration. This could be attributed to further growth of nanoparticles forming large particles or particle aggregation to form bigger units [16]; [15]. Similar results on increase in quantity of nanoparticles with time followed by a decrease in levels of nanoparticles beyond the optimum time has been reported by have been reported in literature [17]; [18].

3.1.2 Influence of quantity of keratin on synthesis of KE-CuNPs

Copper nanoparticles yield increased with increase in amount of keratin precipitate as presented in Fig. 2 (b). Maximum yield was obtained using 1 g of keratin. The yield decreased with further increase in amount of keratin used. Smaller quantities of keratin were not sufficient to reduce all Cu^{2+} to Cu^0 this resulted in lower yield [17]. When larger quantity of keratin is used, there was further growth of nanoparticles or aggregation of nanoparticles to form larger nanoparticles [19].

3.1.3 Effect of Copper (II) Sulphate Concentration on Synthesis of Copper Nanoparticle

Results on effect of Copper (II) Sulphate concentration on synthesis of copper nanoparticle are displayed in Fig. 2 c. The yield of Copper nanoparticles reduced with upsurge of copper sulphate concentration, this could be ascribed to the point that when the concentration of copper (II) sulphate is increased, the nanoparticles formed aggregate to form larger particles which precipitate [19]. Growth of nanoparticles to larger particles results in bathochromic shift to longer wavelength [16]. Similar results were reported in synthesis of collagen based AgNPs for biological use and characterization [19] and in synthesis of CuNps using *Senna didymobotrya* [20].

3.1.4 Effect of Temperature on Synthesis of Copper Nanoparticles

Temperature affects bio reduction of metal ions. Ambient temperature is required in biosynthesis of nanoparticles for maximum yield [21]. Some metabolites reduce metal ions at elevated temperature [16]. Fig. 2 d shows results on the impact of temperature on synthesis of CuNps using keratin. The quantity of copper nanoparticles obtained increased with increase in

Preprint not peer reviewed

This preprint research paper has not been peer reviewed. Electronic copy available at: https://ssrn.com/abstract=4957961

temperature. At lower temperature, there is agglomeration of nanoparticles [20]. At elevated temperature, crystal growth rate increases [21]. Similar outcomes were observed by Sadia et al, in synthesis of CuNps by *Senna didymobotrya* root extract [20].

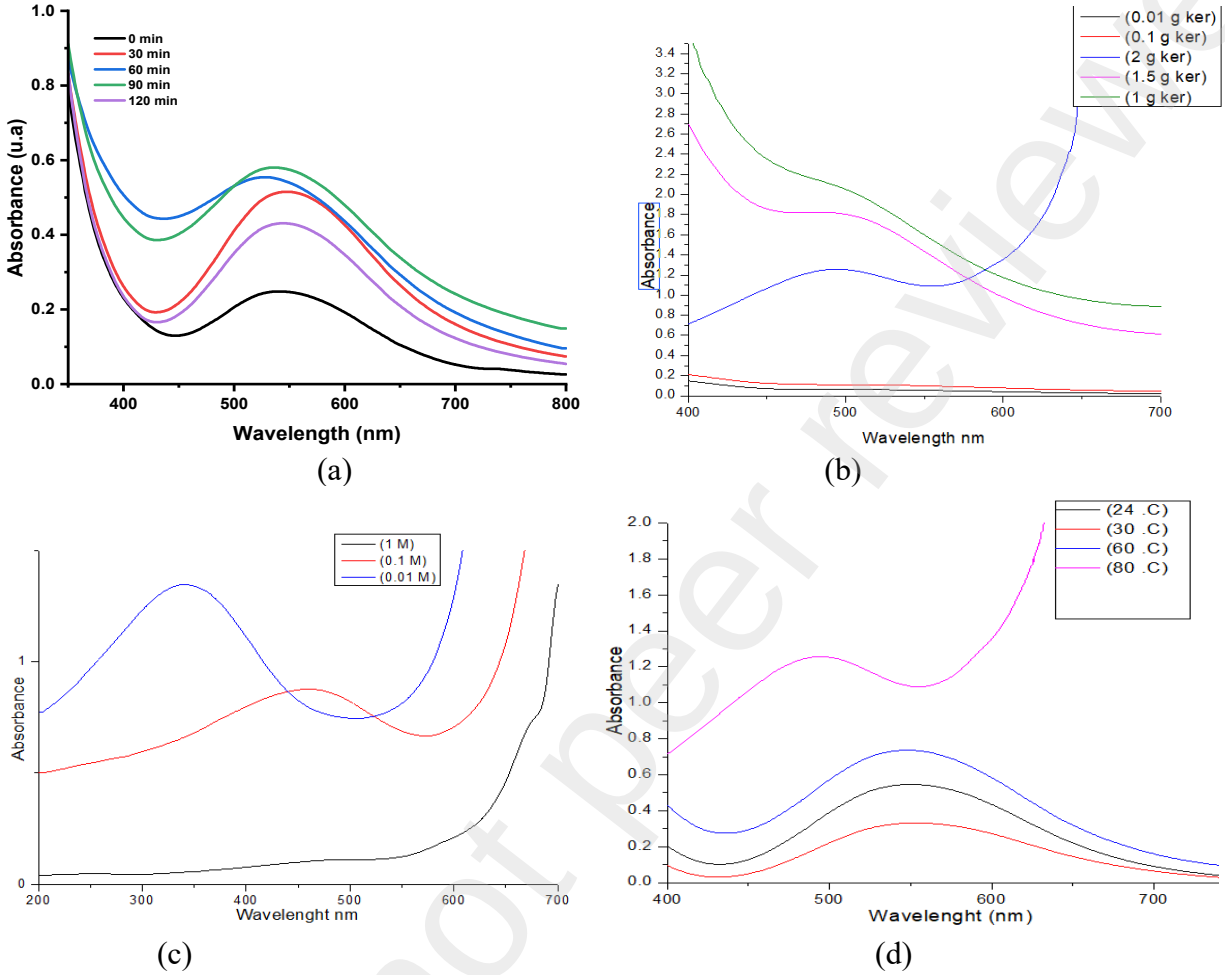
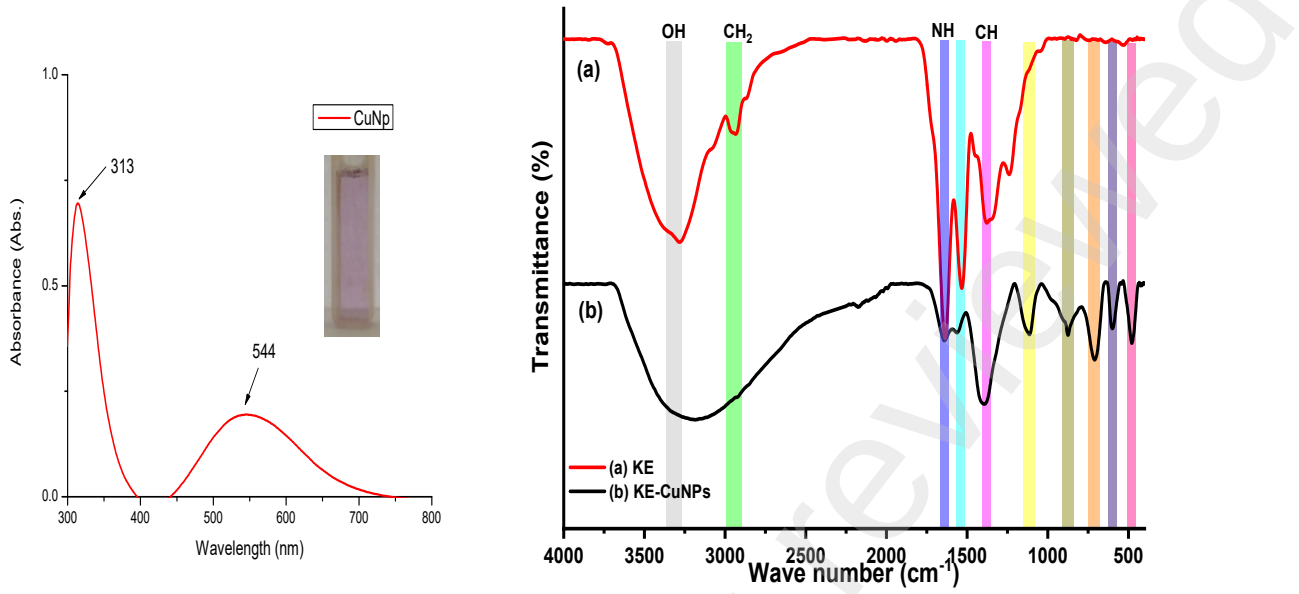


Fig. 2: Effect of (a) Reaction time (b) Quantity of keratin (c) concentration of copper ions and (d) temperature on the synthesis of copper nanoparticles.

3.2 Characterization of copper nanoparticles

Formation of CuNps was marked with the appearance of a violet color. UV-vis scan 300 nm-800 nm was done using UV-1800 Shimadzu spectrometer. Two main peaks at 313 nm and 544 nm signified formation of copper nanoparticles as displayed by Fig. 3a. FT-IR spectrum (Fig. 3b) of synthesized copper nanoparticles shows existence of O-H, C□C, C-O functional groups on nanoparticles indicating involvement of keratin biomolecules in formation of CuNp . Absorption peak at 1397 cm^{-1} is linked to $C-H$ bending vibrations in the bio molecules [22]. Amide 1 band obtained at 1646 cm^{-1} is associated with $C=O$ stretching [23]. Absorption band obtained at 3150 cm^{-1} correlate with N-H or O-H stretching [24]. Absorption band at 1397 cm^{-1} is due to O-H stretching. The absorption band obtained at 1118 cm^{-1} is associated with C-O stretching [22].The results are presented in Table 1.

This preprint research paper has not been peer reviewed. Electronic copy available at: https://ssrn.com/abstract=4957961



(a) (b)

Fig. 3: (a) UV-vis spectrometer scan and (b) FT-IR spectrum for copper nanoparticles solution.

X-Ray diffraction (XRD) analysis results for copper are presented in Fig. 4. The results indicate an intense peak at 43.3° which corresponds to fcc plane (111). This matches fcc of bulk copper [25]. The peak at 50 corresponds to (200) fcc structure. The peak at 73.7 corresponds to (220) fcc plane. Small peaks at 90 and 94.7 matched fcc planes (311) and (222) respectively. These peaks matched fcc structure of copper [26].

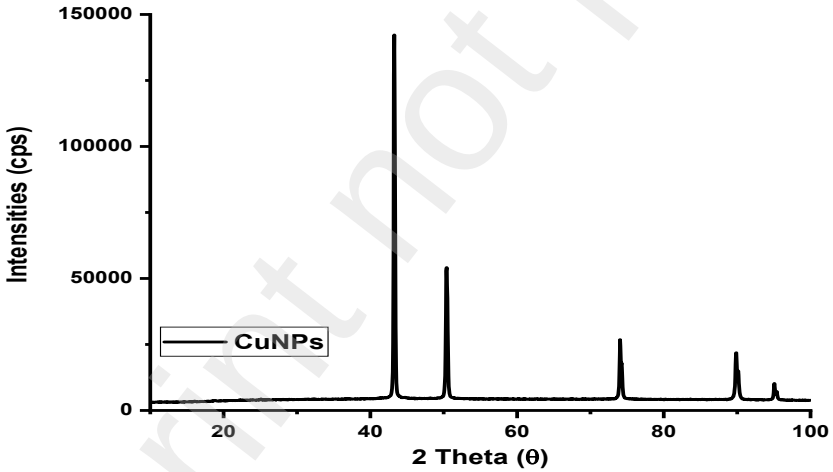
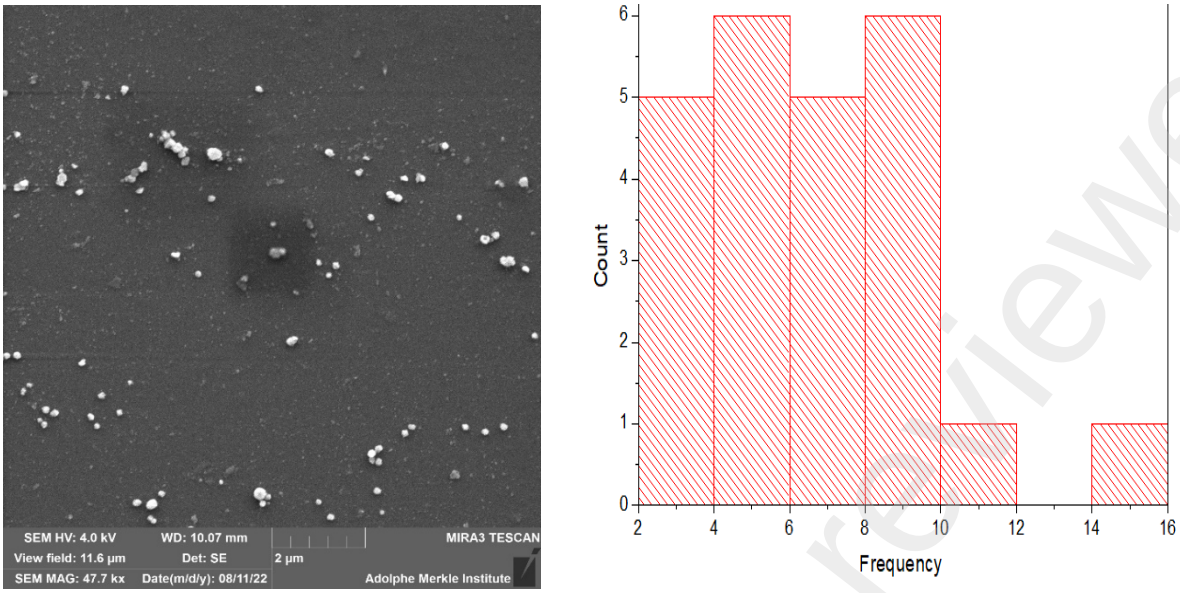


Fig. 4: XRD pattern for copper nanoparticles

Scanning Electron Microscopy (SEM) analysis was performed on CuNps to ascertain the surface morphology and the size of nanoparticles. SEM image for the CuNps presented at a magnification of 47700X (Fig 5. a) indicates non agglomerated spherical shaped CuNps. The dimensions dispersal analysis (Fig. 5b) displays that the dimensions range for copper nanoparticles attained was within the range of 2 nm-16 nm.

Preprint not peer reviewed

This preprint research paper has not been peer reviewed. Electronic copy available at: https://ssrn.com/abstract=4957961



(a) (b)

Fig. 5: (a) SEM image for CuNps (b) Image size distribution for CuNps

3.3 Adsorption Experiments

3.3.1 Influence of time on adsorption of Methylene blue dye by copper nanoparticles

Interaction period between adsorbent and adsorbate is crucial for cost estimation in designing large scale industrial adsorption system [1]. Influence of time was explored by monitoring changes in concentration of MB dye from 0 min to 360 min at 25 °C (Fig.6). Quantity of dye removed augmented with time increase. Adsorption rate was high at the beginning of the experiment with 54% of the MB dye adsorbed within the first 30 minutes. High rate of adsorption within the first 30 minutes was due to a large surface area of the nanoparticles and numerous sorption sites at the beginning of the experiment [13]. Equilibrium was attained after 330 minutes with 95 % of the dye removal attained, when the adsorption sites on the nanoparticles became saturated [27]. Once equilibrium has been reached, the remaining adsorption sites will no longer take any dye molecules due to electrostatic forces of repulsion between molecules bound on occupied binding sites on nanoparticles and the dye molecules in aqueous phase [4]. This is similar to findings which have been reported on adsorption of dyes [27].

Preprint not peer reviewed

This preprint research paper has not been peer reviewed. Electronic copy available at: https://ssrn.com/abstract=4957961

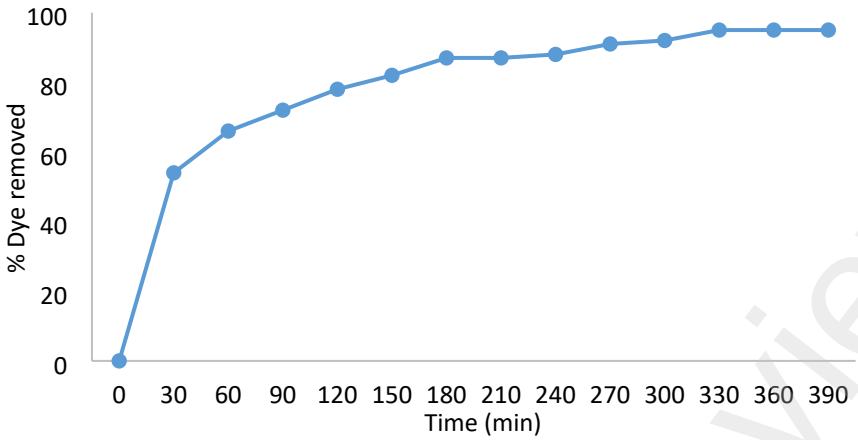


Fig. 6: Influence of time on adsorption of MB by copper nanoparticles (MB 5ppm, CuNps 8mg/10 ml at 25°C).

3.3.2 Effect of Copper Nanoparticles dose

Adsorbent dose is a vital factor which affect sorption since the process depends on accessibility of binding sites and surface area on the adsorbent [13]. Influence of quantity of CuNp was evaluated by altering the quantity of CuNps used from 2 mg – 12 mg (Fig. 7). Efficiency of MB removal improved with rise in quantity of CuNps used. The efficiency of dye removal at equilibrium improved from 4.925 mg/g to 5.899 mg/g when the quantity of copper nanoparticles rose from 1 mg to 8 mg. This is owed to increased number of active adsorption sites and adsorption bores as the quantity of copper nanoparticles is increased [27]. Efficiency of dye removal decreased with further increase in amount of nanoparticles to 5.864 mg/g when 10 mg of copper nanoparticles was used. This is due to aggregation of nanoparticles which decreases surface area for adsorption and increase diffusion path length [28]. Similar outcomes were observed in removal of MB using activated carbon, in which at high adsorbent dosages, the adsorption capacity decreased [27].

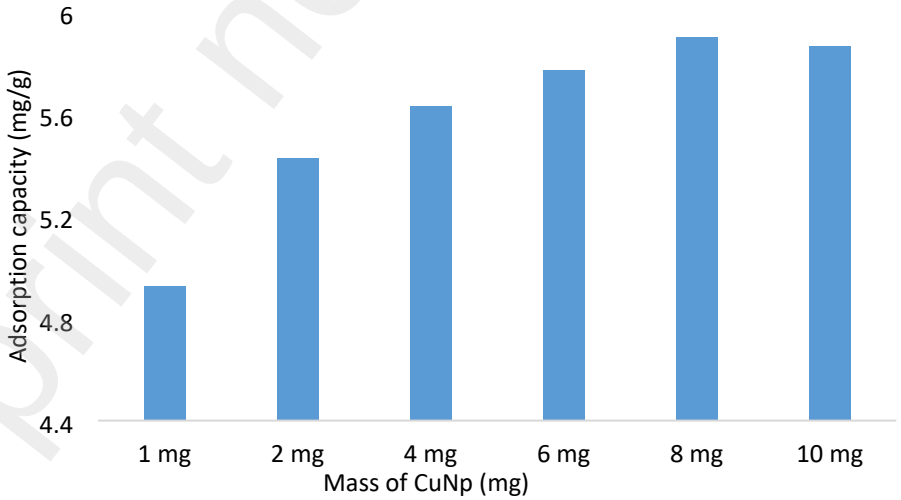


Fig. 7: Copper nanoparticles dose on sorption of Methylene Blue dye (MB 5ppm at 25 °C).

Preprint not peer reviewed

This preprint research paper has not been peer reviewed. Electronic copy available at: https://ssrn.com/abstract=4957961

3.3.3 Effect of Methylene Blue Concentration

Influence of preliminary of MB dye concentration was evaluated by altering initial of MB dye concentration from 0.625 ppm – 10 ppm at 25 °C (Fig. 8). The quantity of MB removed per unit mass of CuNps at equilibrium surged from 0.75217 mg/g to 12.01 mg/g when initial concentration of methylene blue rose from 0.625 ppm to 10 ppm. This is because of an increase in concentration gradient as dye concentration increases increasing the driving force opposition to mass transfer of the dye molecules from bulk to the surface of nanoparticles is overcome by the driving force hence more molecules are adsorbed [29]. Increasing concentration of MB will also increase the interactivity between the dye molecules and copper nanoparticles [30]. For instance when 0.625 ppm was used, equilibrium was attained after 180 minutes, while adsorption process attained equilibrium after 360 minutes when 10 ppm was used. Similar observation were recorded in sorption of MB using activated carbon [27].

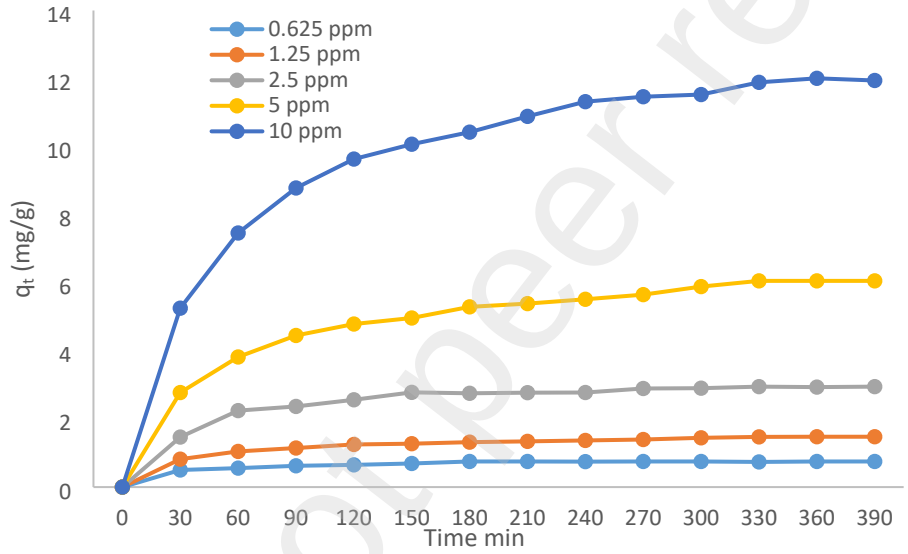


Fig 8: Influence of dye concentration on adsorption of MB by copper nanoparticles (CuNps 8 mg/10 ml of the dye at 25°C)

3.3.4 Influence of pH on sorption of MB

Change in pH affects adsorption of dyes significantly hence it is one of the factors considered in sorption [5]. It affects the level of ionization of basic and acidic compounds [27]. pH change alters the surface charge on adsorbent [31]. Influence of pH on sorption of MB by copper nanoparticles was inspected by changing MB pH from pH 2 to pH 13 at 25°C. Change in adsorption capacity of CuNps was not pronounced over the selected pH range. High adsorption of 96% was attained in acidic conditions with a pH range of 2-5 (Fig. 9). Similar results were reported on MB removal using activated carbon from lemon and orange peels in which maximum removal was attained at pH 5 [32].

Preprint not peer reviewed

This preprint research paper has not been peer reviewed. Electronic copy available at: https://ssrn.com/abstract=4957961

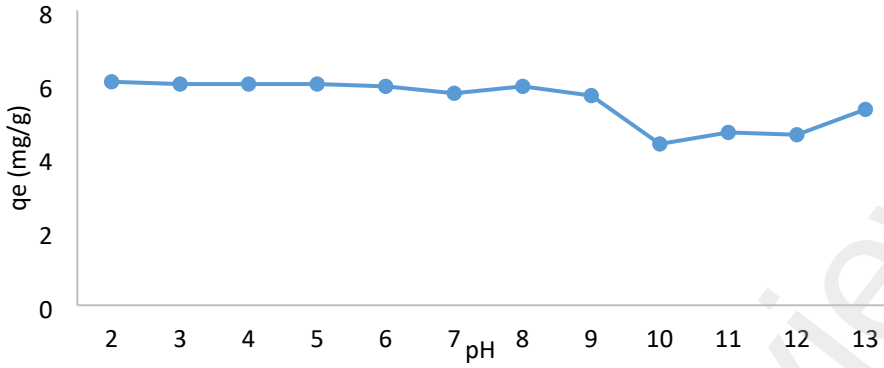


Fig. 9: Influence of pH on adsorption of MB by CuNP (MB 5ppm, CuNP 8 mg/10 ml, at 25 °C)

3.3.5 Influence of temperature on adsorption of MB by copper nanoparticles

Temperature affects the properties of adsorbent surface, dye solubility, flow of dye molecules across boundary layers of the adsorbent and mobility of the dye molecules [33]. Effect of temperature was investigated by conducting adsorption experiment at altered temperature from 25 °C to 60 °C (Fig. 10). There was a small surge in sorption from 6.13 to 6.2436 mg/g on temperature increase from 25 °C to 60 °C. The results point out that methylene blue removal by copper nanoparticles is an endoergic process [34]. Adsorption of methylene blue using activated carbon registered similar findings [27].

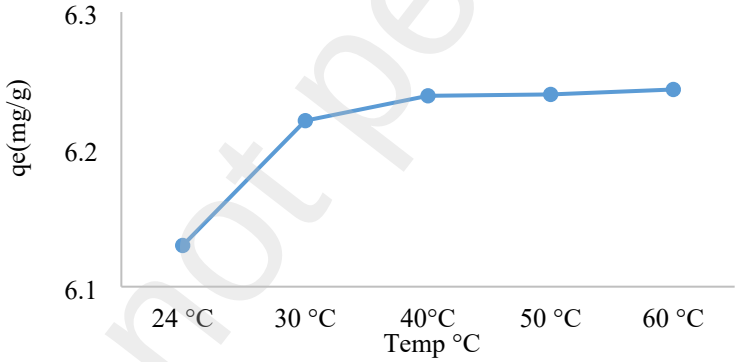


Fig. 10: Influence of temperature on adsorption of MB dye by CuNPs (CuNp 8mg/10 ml of MB dye 5 ppm)

3.4 Adsorption Kinetics

Adsorption kinetics was used to study rate of reactions between the MB and the copper nanoparticles and the conditions which affect their rate of reaction. The data obtained in experiment were fitted to Pseudo first and second order kinetics. The Pseudo first order kinetics equation is presented in equ 3.

$$\log (q_e - q_t) = \log q_e - \frac{tk_1}{2.303} \quad (3)$$

k_1 is the rate constant for adsorption in the pseudo first order model equation. q_e and q_t represents the quantity of methylene blue dye removed by copper nanoparticles at equilibrium and time (t) respectively. A graph of log $(q_e - q_t)$ versus t was plotted as shown in Fig. 11 (a)

Preprint not peer reviewed

This preprint research paper has not been peer reviewed. Electronic copy available at: https://ssrn.com/abstract=4957961

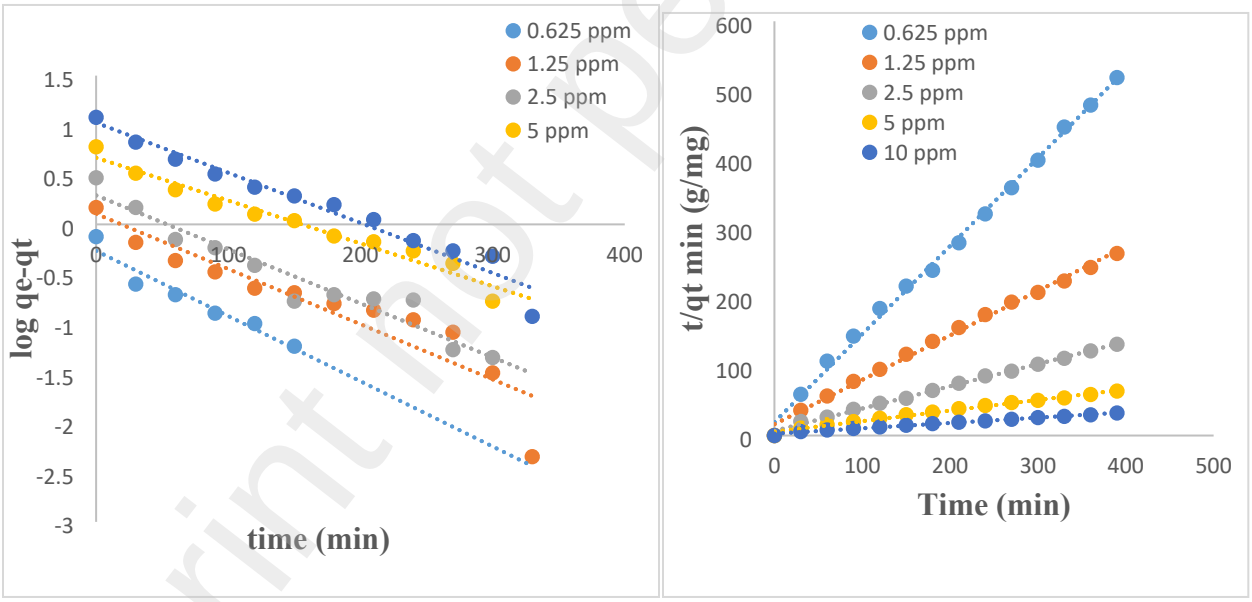
and used to find out values of k_1 and q_e from the slope and the y intercept respectively. Pseudo second order equation is presented in equ 4.

$$\frac{t}{q_t} = \frac{1}{k_2} \cdot \frac{1}{q_e^2} + \frac{t}{q_e} \quad (4)$$

A graph of $\frac{t}{q_t}$ against t is presented in Fig. 11(b). From the gradient of the graph and the $\frac{t}{q_t}$ intercept q_e and k_2 the rate constant for pseudo second order adsorption in g/mg/min were determined basing on the equation of a line. From the graph, a higher value of correlation efficient (R^2 values ranging between 0.9904 and 0.9971) were attained indicating Pseudo second order model is appropriate for explaining sorption of MB by copper nanoparticles. Table 1 presents the results obtained from the plotted graphs.

Table 1: Parameters for first and second order Pseudo kinetics studies

Pseudo First order models parameters					Pseudo second order models parameters		
MB (ppm)	$q_{e\,(exp)}$(g^{1}mg)	$q_{e\,calc}$(g^{1}mg)	k_1 (gmg^{-1}min^{-1})	R^2	$q_{e\,calc}$(mg/g)	k_2(g mg^{-1}min^{-1})	R^2
0.625	0.7522	0.5411	0.001520	0.9356	0.7839	0.08414	0.9969
1.25	1.479	1.276	0.01290	0.8602	1.5540	0.02535	0.9947
2.5	2.951	1.960	0.01244	0.9377	3.0989	0.01529	0.9963
5	6.057	4.699	0.009903	0.9625	6.5190	0.004304	0.9904
10	12.01	10.60	0.01175	0.9577	12.940	0.002208	0.9971



(a) (b)

Figure 11: (a) Plots for Pseudo first order kinetics (b) Pseudo second order kinetics

3.5 Adsorption Isotherm

Adsorption is a dual step process which involving pollutant molecules getting attached to the adsorbent sites and desorbed. Dynamic equilibrium is attained when the rates of the two processes are the comparable. Langmuir and Freundlich isotherms were applied in describing connection amid equilibrium concentration C_e of MB in solution and the amount of colorant

This preprint research paper has not been peer reviewed. Electronic copy available at: https://ssrn.com/abstract=4957961

removed at equilibrium. Langmuir model presume that the adsorbent surface is homogeneous and the arrangement of pollutant particles on adsorbent surface forms a single layer on energy comparable sites [27]. Linearized forms of Langmuir model are presented in equ 5.

$$\frac{1}{q_e} = \frac{1}{q_{ax} b C_e} + \frac{1}{q_{ax}} \quad (5)$$

q_e (g^{-1} mg) is the amount of the contaminant molecules removed at equilibrium, C_e is the equilibrium concentration for the colorant molecules in solution. q_{ax} (g^{-1} mg) represents the highest coverage capacity for the monolayer on the adsorbent exterior, b (mg^{-1} L) is a Langmuir constant displays attraction for the active sites. From the graph of $\frac{1}{q_e}$ vs $\frac{1}{C_e}$, the values of q_{ax} and b are gotten from the gradient and $\frac{1}{q_e}$ intercept correspondingly [4]. On further survey, separation factor R_L used to determine the favorability of the sorption process was calculated using equ 6.

$$R_L = \frac{1}{bC_o + 1} \quad (6)$$

C_o is the highest preliminary concentration used. Values of R_L defines if the isotherm is non reversible, if (R_L=0), satisfactory (If the value is greater than 0, but lower than 1), non-satisfactory (R_L >1) or rectilinear (R_L= 1)[27]. R_L values obtained (0.1850-0.7842) was lower than unity but greater than 0 indicating a satisfactory adsorption process.

Freundlich isotherm considers adsorption surface to be a multilayer progression in which interlayers and adsorbent surface forms heterogeneous system [35]. Freundlich equation is presented in equ 7:

$$\log q_e = \log K_F + \frac{1}{n} \log C_e \quad (7)$$

K_F (mg/g)(L/mg) and 1/n signifies the Freundlich isotherm constants. $\frac{1}{n}$ Characterizes sorption intensity on adsorbent surface. The value of $\frac{1}{n}$ should be between 0.1 and 1 which correspond to (n≥1) for a satisfactory adsorption procedure [13]. From the plots of log q_e against log C_e values of K_F, which indicates approximate adsorption capacity and $\frac{1}{n}$ are attained from the log q_e intercept and the slope respectively. When the value of n is above 1, it point out a satisfactory adsorption progression. The values of Langmuir and Freundlich parameters: q_{ax} , b, R_L, n and K_F were determined and tabulated in Table 2. From the results, both R^2 value for Langmuir and Freundlich isotherm were almost equal signifying that both models could describe adsorption at tested temperature of 25°C.

Table 2: Langmuir and Freundlich isotherm constants for adsorption of MB dye on CuNps

Langmuir adsorption isotherm				Freundlich adsorption isotherm		
q_{max}	b	R^2	R_L	K_F	*n*	R^2
14.53	0.4404	0.9589	0.1850	20.6538	1.085	0.9585

This preprint research paper has not been peer reviewed. Electronic copy available at: https://ssrn.com/abstract=4957961

3.6 Thermodynamic Studies

Study of thermodynamic behavior on variables which include enthropy change ΔS° (J/kg/mol), Gibbs free energy change and enthalpy change were examined by carrying out adsorption at various temperatures including 297 K, 303K, 313K, 323K and 333K and using the Vant hoff equation 8 given below

$$\Delta G^\circ = -RT\ln K \quad (8)$$

$$-RT\ln K = \Delta H^\circ - T\,\Delta G^\circ \quad (9)$$

$$\ln K = -\frac{\Delta H^\circ}{RT} + \frac{\Delta S^\circ}{R} \quad (10)$$

K is the distribution coefficient for adsorption which describes colorant concentration on solid phase to the concentration of the dye in aqueous phase at equilibrium. T is the absolute temperature used to carry out the investigation. R depicts the gas constant (8.314 J/K/mol). Graphical representation plotted for ln K against absolute temperature is presented in Fig. 12.

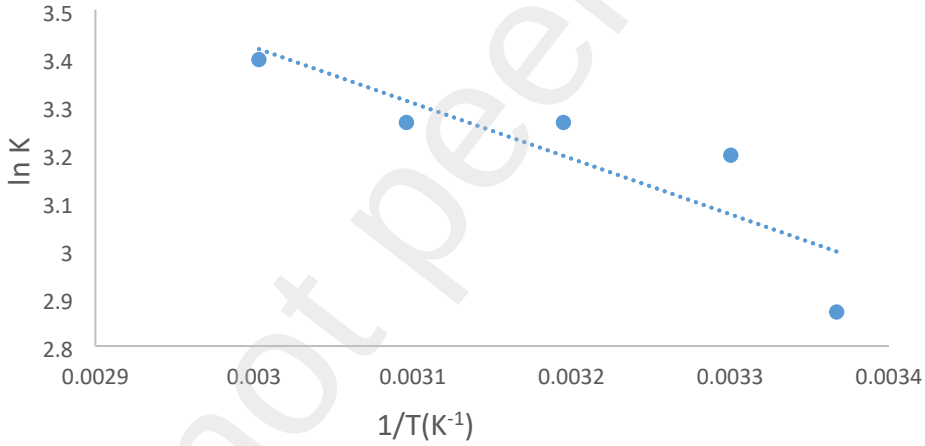


Fig. 12: Plots for ln K against $\frac{1}{T}$ (K^{-1})

Thermodynamic parameters were determined and displayed in Table 3. The negative values of ΔG° specify impulsiveness and feasibility of adsorption of MB on CuNps. Positive ΔS° specifies that the randomness of solution/solid interface augmented all through sorption progression [27]. ΔH° is positive hence the process is endothermic [36]. The magnitude is lower than 20 (KJ/mol) signifying a physisorption procedure governed by van der waals forces [1].

Table 3: Thermodynamic parameters for MB dye adsorption on CuNp.

ΔG^0(kJ/mol)					ΔH^0 (kJ/mol)	ΔS^0 (J/K/mol)	R^2
297K	303K	313K	323K	333K			
-7.399	-7.743	-8.316	-8.889	-9.462	+9.622	+0.05731	0.7531

Preprint not peer reviewed

This preprint research paper has not been peer reviewed. Electronic copy available at: https://ssrn.com/abstract=4957961

4. CONCLUSION

Keratin is a suitable for use as a reducing and capping agent in synthesis of copper nanoparticles. The optimum conditions for synthesis of CuNps were a time of 90 minutes, 1 g of keratin in 50 ml of $CuSO_4$, 0.01M Cu^{2+} and a temperature of 80 °C. The nanoparticles were suitable for use in adsorptive removal of MB dye from aqueous media. FT-IR characterization revealed that CuNps associated with O-H, C=C, C-O groups. XRD measurement showed FCC crystalline structure of CuNps. SEM measurements showed spherical nanoparticles with particle size ranging between 2 -16 nm. Batch adsorption experiments established that adsorption process was highly controlled by operative conditions which included contact time, quantity of adsorbent, concentration, pH and temperature. Adsorption of dye at room temperature attained equilibrium after 330 minutes with 95 % dye removal attained. The sorption capacities improved with upsurge in temperature and dye concentration. The optimal condition for MB dye sorption was a pH range of 2-5 and a dosage of 8 mg/10 ml of the dye. Both Langmuir and Freundlich isotherm were almost equal signifying that both models could describe adsorption process at tested temperature of 25°C. Pseudo second order kinetics was suitable in describing sorption process while adsorption isotherms revealed that the process followed Temkins isotherm model.

REFERENCES

[1] Cheruiyot, G. K., Wanyonyi, W. C., Kiplimo, J. J., and Maina, E. N., 2019, "Adsorption of Toxic Crystal Violet Dye Using Coffee Husks: Equilibrium, Kinetics and Thermodynamics Study," Sci. Afr., **5**, p. e00116.

[2] Wekoye, J. N., Wanyonyi, W. C., Wangila, P. T., and Tonui, M., 2020, "Kinetic and Equilibrium Studies of Congo Red Dye Adsorption on Cabbage Waste Powder," Environ. Chem. Ecotoxicol., p. S2590182620300047.

[3] Li, H., Budarin, V. L., Clark, J. H., North, M., and Wu, X., 2022, "Rapid and Efficient Adsorption of Methylene Blue Dye from Aqueous Solution by Hierarchically Porous, Activated Starbons®: Mechanism and Porosity Dependence," J. Hazard. Mater., **436**, p. 129174.

[4] Wanyonyi, W. C., Onyari, J. M., and Shiundu, P. M., 2014, "Adsorption of Congo Red Dye from Aqueous Solutions Using Roots of Eichhornia Crassipes: Kinetic and Equilibrium Studies," Energy Procedia, **50**, pp. 862–869.

[5] Wu, Y., 2017, "The Removal of Methyl Orange by Periphytic Biofilms," *Periphyton*, Elsevier, pp. 367–387.

[6] Oladoye, P. O., Ajiboye, T. O., Omotola, E. O., and Oyewola, O. J., 2022, "Methylene Blue Dye: Toxicity and Potential Elimination Technology from Wastewater," Results Eng., **16**, p. 100678.

[7] Othman, N. H., Alias, N. H., Shahruddin, M. Z., Abu Bakar, N. F., Nik Him, N. R., and Lau, W. J., 2018, "Adsorption Kinetics of Methylene Blue Dyes onto Magnetic Graphene Oxide," J. Environ. Chem. Eng., **6**(2), pp. 2803–2811.

[8] Ramsay, R. R., Dunford, C., and Gillman, P. K., 2007, "Methylene Blue and Serotonin Toxicity: Inhibition of Monoamine Oxidase A (MAO A) Confirms a Theoretical Prediction," Br. J. Pharmacol., **152**(6), pp. 946–951.

[9] Wanyonyi, W. C., Onyari, J. M., and Shiundu, P. M., 2013, "Adsorption of Methylene Blue Dye from Aqueous Solutions Using Eichhornia Crassipes," Bull. Environ. Contam. Toxicol., **91**(3), pp. 362–366.

[10] Kuang, Y., Guo, X., Hu, J., Li, S., Zhang, R., Gao, Q., Yang, X., Chen, Q., and Sun, W., 2020, "Occurrence and Risks of Antibiotics in an Urban River in Northeastern Tibetan Plateau," Sci. Rep., **10**(1), p. 20054.

This preprint research paper has not been peer reviewed. Electronic copy available at: https://ssrn.com/abstract=4957961

[11] Adeola, A. O., and Forbes, P. B. C., 2021, "Advances in Water Treatment Technologies for Removal of Polycyclic Aromatic Hydrocarbons: Existing Concepts, Emerging Trends, and Future Prospects," Water Environ. Res., **93**(3), pp. 343–359.
[12] Chakraborty, S., Mukherjee, A., Das, S., Raju Maddela, N., Iram, S., and Das, P., 2020, "Study on Isotherm, Kinetics, and Thermodynamics of Adsorption of Crystal Violet Dye by Calcium Oxide Modified Fly Ash," Environ. Eng. Res., **26**(1).
[13] Sabna, V., Thampi, S. G., and Chandrakaran, S., 2016, "Adsorption of Crystal Violet onto Functionalised Multi-Walled Carbon Nanotubes: Equilibrium and Kinetic Studies," Ecotoxicol. Environ. Saf., **134**, pp. 390–397.
[14] Singh, S., Kumar, V., Romero, R., Sharma, K., and Singh, J., 2019, "Applications of Nanoparticles in Wastewater Treatment," p. 24.
[15] Patra, J. K., and Baek, K.-H., 2014, "Green Nanobiotechnology: Factors Affecting Synthesis and Characterization Techniques," J. Nanomater., **2014**, pp. 1–12.
[16] Lukman, A. I., Gong, B., Marjo, C. E., Roessner, U., and Harris, A. T., 2011, "Facile Synthesis, Stabilization, and Anti-Bacterial Performance of Discrete Ag Nanoparticles Using Medicago Sativa Seed Exudates," J. Colloid Interface Sci., **353**(2), pp. 433–444.
[17] Bhavyasree, P. G., and Xavier, T. S., 2022, "Green Synthesised Copper and Copper Oxide Based Nanomaterials Using Plant Extracts and Their Application in Antimicrobial Activity: Review," Curr. Res. Green Sustain. Chem., **5**, p. 100249.
[18] Qomariyah, A., and Hakim, A. K., 2024, "Synthesis of Copper Nanoparticles Using Dragon Fruit (Hylocereus Polyrhizus) Extract as a Bio- Reductor and Their Analysis Using a UV-Visible Spectrophotometer."
[19] Cardoso, V. S., Quelemes, P. V., Amorin, A., Primo, F. L., Gobo, G. G., Tedesco, A. C., Mafud, A. C., Mascarenhas, Y. P., Corrêa, J. R., Kuckelhaus, S. A., Eiras, C., Leite, J. R. S., and Silva, D., 2014, "Collagen-Based Silver Nanoparticles for Biological Applications: Synthesis and Characterization," p. 9.
[20] Sadia, B. O., Cherutoi, J. K., and Achisa, C. M., 2021, "Optimization, Characterization, and Antibacterial Activity of Copper Nanoparticles Synthesized Using Senna Didymobotrya Root Extract," J. Nanotechnol., **2021**, pp. 1–15.
[21] Keat, C. L., 2015, "Biosynthesis of Nanoparticles and Silver Nanoparticles," Bioresour. Bioprocess., **2**, p. 11.
[22] Amaliyah, S., Pangesti, D. P., Masruri, M., Sabarudin, A., and Sumitro, S. B., 2020, "Green Synthesis and Characterization of Copper Nanoparticles Using Piper Retrofractum Vahl Extract as Bioreductor and Capping Agent," Heliyon, **6**(8), p. e04636.
[23] Vahur, S., Teearu, A., Peets, P., Joosu, L., and Leito, I., 2016, "ATR-FT-IR Spectral Collection of Conservation Materials in the Extended Region of 4000-80 Cm–1," Anal. Bioanal. Chem., **408**(13), pp. 3373–3379.
[24] Göl, F., Aygün, A., Seyrankaya, A., Gür, T., Yenikaya, C., and Şen, F., 2020, "Green Synthesis and Characterization of Camellia Sinensis Mediated Silver Nanoparticles for Antibacterial Ceramic Applications," Mater. Chem. Phys., **250**, p. 123037.
[25] Suramwar, N. V., Thakare, S. R., and Khaty, N. T., 2016, "One Pot Synthesis of Copper Nanoparticles at Room Temperature and Its Catalytic Activity," Arab. J. Chem., **9**, pp. S1807–S1812.
[26] Thiruvengadam, M., Chung, I.-M., Gomathi, T., Ansari, M. A., Gopiesh Khanna, V., Babu, V., and Rajakumar, G., 2019, "Synthesis, Characterization and Pharmacological Potential of Green Synthesized Copper Nanoparticles," Bioprocess Biosyst. Eng., **42**(11), pp. 1769–1777.
[27] Zhang, X., Kuang, Y., and Zhou, S., 2020, "Adsorption of Methylene Blue in Water onto Activated Carbon by Surfactant Modification," Water, **12**(2), p. 587.
[28] Adeyemo, A. A., Adeoye, I. O., and Bello, O. S., 2017, "Adsorption of Dyes Using Different Types of Clay: A Review," Appl. Water Sci., **7**(2), pp. 543–568.

Preprint not peer reviewed

This preprint research paper has not been peer reviewed. Electronic copy available at: https://ssrn.com/abstract=4957961

[29] Mutunga, M. F., Wanyonyi, W. C., and Ongera, G., 2020, "Utilization of Macadamia Seed Husks as a Low-Cost Sorbent for Removing Cationic Dye (Basic Blue 3 Dye) from Aqueous Solution," Environ. Chem. Ecotoxicol., **2**, pp. 194–200.
[30] Dahri, M. K., Kooh, M. R. R., and Lim, L. B. L., 2013, "Removal of Methyl Violet 2B from Aqueous Solution Using *Casuarina Equisetifolia* Needle," ISRN Environ. Chem., **2013**, pp. 1–8.
[31] Khan, I., Saeed, K., Zekker, I., Zhang, B., Hendi, A. H., Ahmad, A., Ahmad, S., Zada, N., Ahmad, H., Shah, L. A., Shah, T., and Khan, I., 2022, "Review on Methylene Blue: Its Properties, Uses, Toxicity and Photodegradation," Water, **14**(2), p. 242.
[32] Ramutshatsha-Makhwedzha, D., Mavhungu, A., Moropeng, M. L., and Mbaya, R., 2022, "Activated Carbon Derived from Waste Orange and Lemon Peels for the Adsorption of Methyl Orange and Methylene Blue Dyes from Wastewater," Heliyon, **8**(8), p. e09930.
[33] Wekoye, J. N., Wanyonyi, W. C., and Wangila, P. T., 2023, "Adsorption of Recalcitrant Malachite Green Dye from Aqueous Solution Using Cabbage Waste Powder," Metz, France, p. 020002.
[34] Liu, L., Zhang, X., Yang, L., Ren, L., Wang, D., and Ye, J., 2017, "Metal Nanoparticles Induced Photocatalysis," Natl. Sci. Rev., **4**(5), pp. 761–780.
[35] Mohammad, N., and Atassi, Y., 2020, "Adsorption of Methylene Blue onto Electrospun Nanofibrous Membranes of Polylactic Acid and Polyacrylonitrile Coated with Chloride Doped Polyaniline," Sci. Rep., **10**(1), p. 13412.
[36] Piri, F., Mollahosseini, A., Khadir, A., and Milani Hosseini, M., 2019, "Enhanced Adsorption of Dyes on Microwave-Assisted Synthesized Magnetic Zeolite-Hydroxyapatite Nanocomposite," J. Environ. Chem. Eng., **7**(5), p. 103338.

Preprint not peer reviewed

This preprint research paper has not been peer reviewed. Electronic copy available at: https://ssrn.com/abstract=4957961